

The GOGREEN survey: Internal dynamics of clusters of galaxies at redshift 0.9–1.4

A. Biviano^{1,2}, R. F. J. van der Burg³, M. L. Balogh^{4,5}, E. Munari¹, M. C. Cooper⁶, G. De Lucia¹, R. DeMarco⁷, P. Jablonka⁸, A. Muzzin⁹, J. Nantais¹⁰, L. J. Old¹¹, G. Rudnick¹², B. Vulcani¹³, G. Wilson¹⁴, H. K. C. Yee¹⁵, D. Zaritsky¹⁶, P. Cerulo²³, J. Chan¹⁴, A. Finoguenov¹⁷, D. Gilbank^{18,19}, C. Lidman^{20,21}, I. Pintos-Castro¹⁵, and H. Shipley²²

(Affiliations can be found after the references)

1: INAF-Osservatorio Astronomico di Trieste

2: Institute for Fundamental Physics of the Universe, Trieste

Introduction

Is there **A UNIVERSAL DENSITY PROFILE** of clusters?

Navarro, Frenk & White 97:
the mass density profile, $\rho(r)$,
of all cosmological halos,
is **universal** - based on
Cold DM numerical simulations

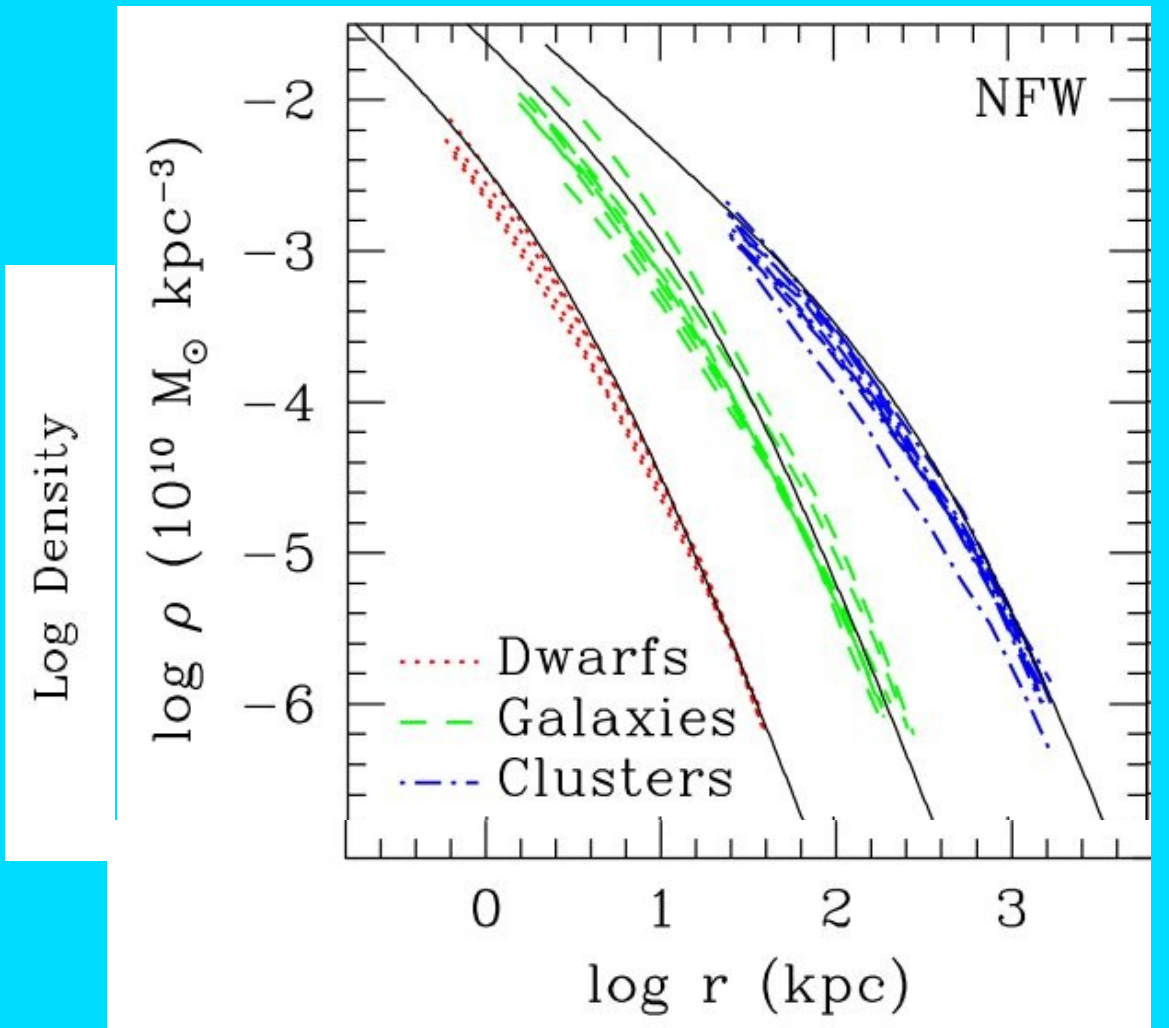
$$\rho(r) \propto (r/r_{-2})^{-1} \times (1 + r/r_{-2})^{-2}$$

$$M(r) = M_{200} \frac{\ln(1 + r/r_{-2}) - r/r_{-2} (1 + r/r_{-2})^{-1}}{\ln(1 + c_{200}) - c_{200}/(1 + c_{200})}$$

2-parameter model:

$$M_{200} \equiv 200 H_z^2 r_{200}^3 / (2 G)$$

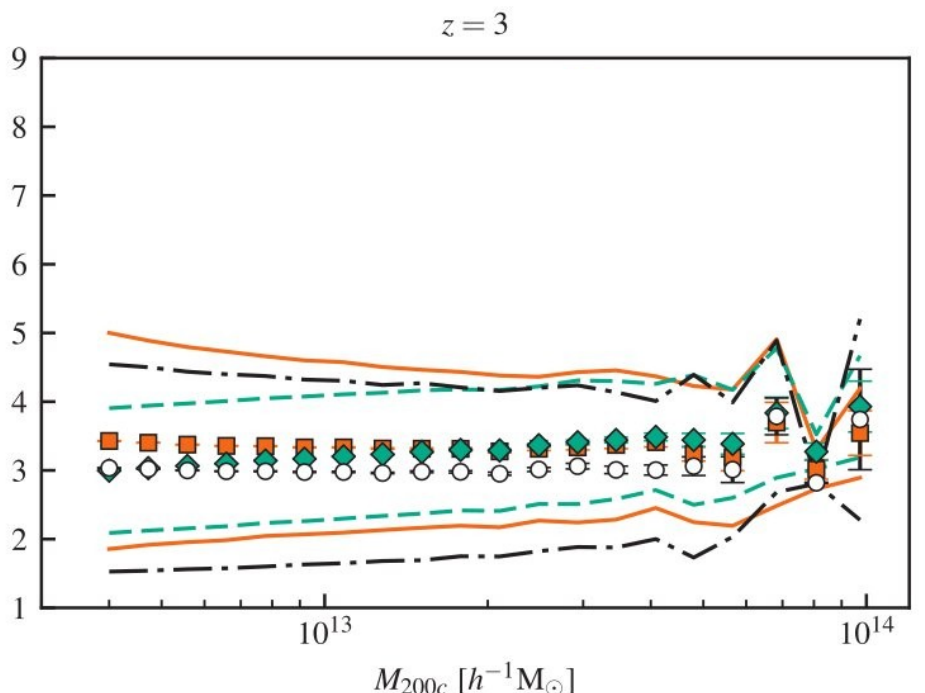
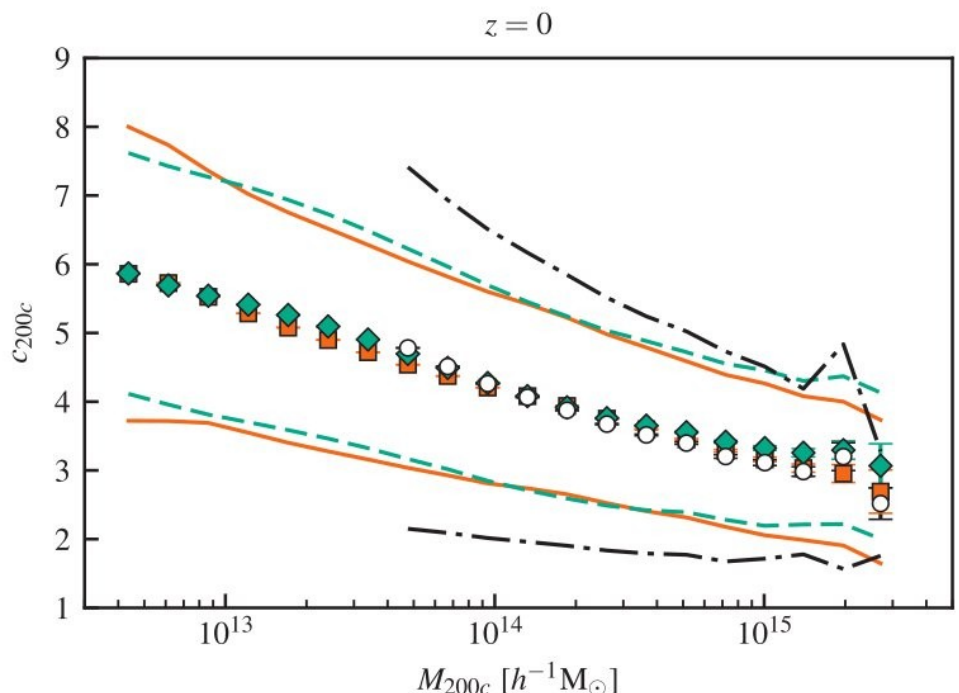
$$c_{200} \equiv r_{200}/r_{-2}$$



(Navarro+04)

Introduction

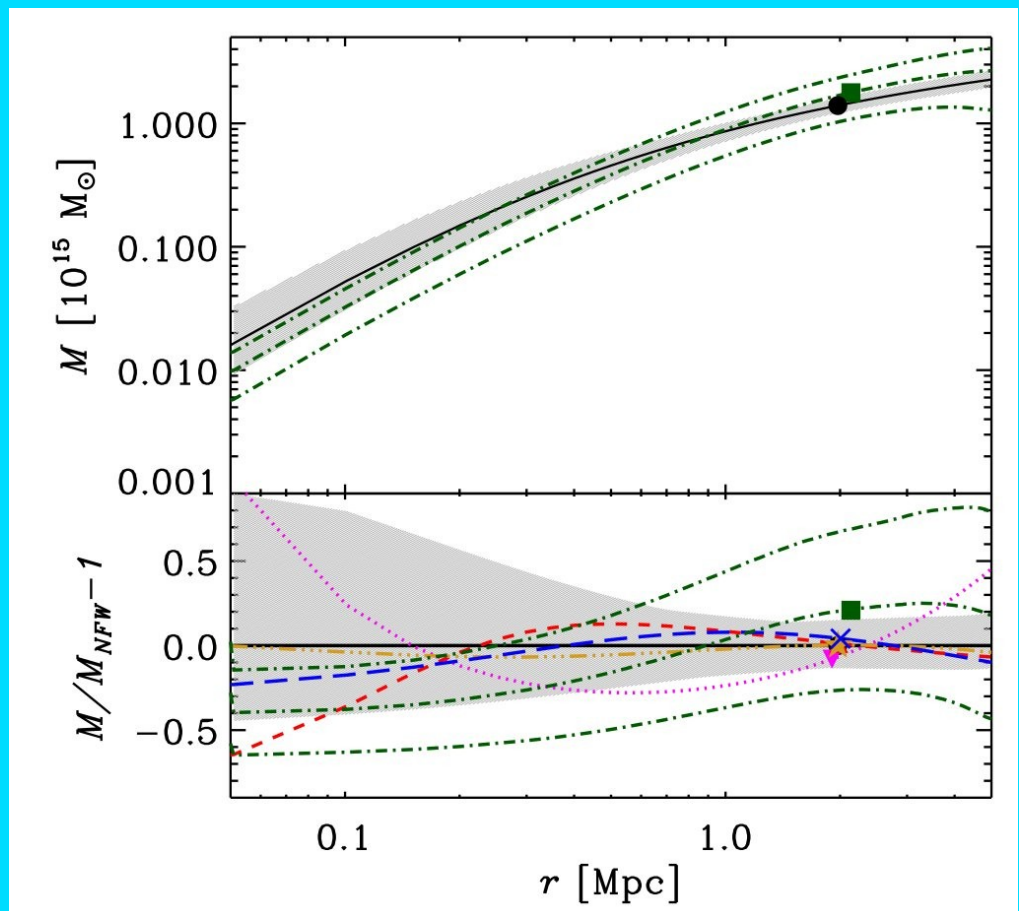
M_{200} and c_{200} are related, and the relation depends on z :



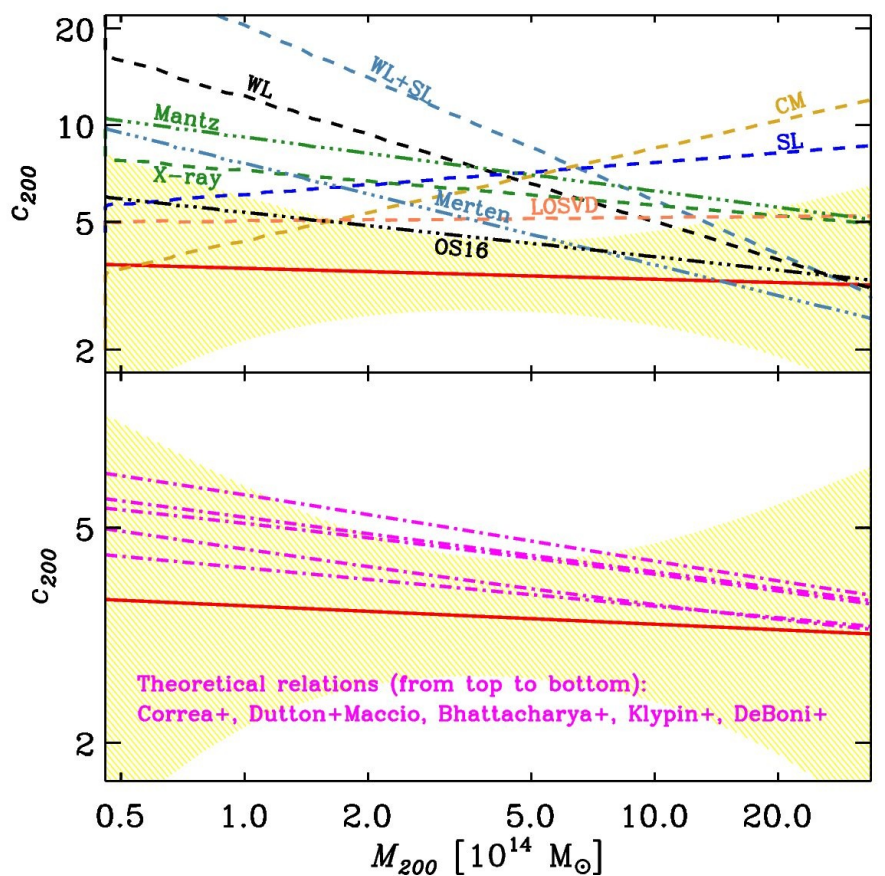
(Child+18, from Λ CDM gravity-only numerical simulations)

Introduction

NFW $M(r)$ model and c_{200} - M_{200} relation verified on real cluster data, mostly at $z < 0.5$



(AB+13, $z=0.44$ cluster from CLASH)

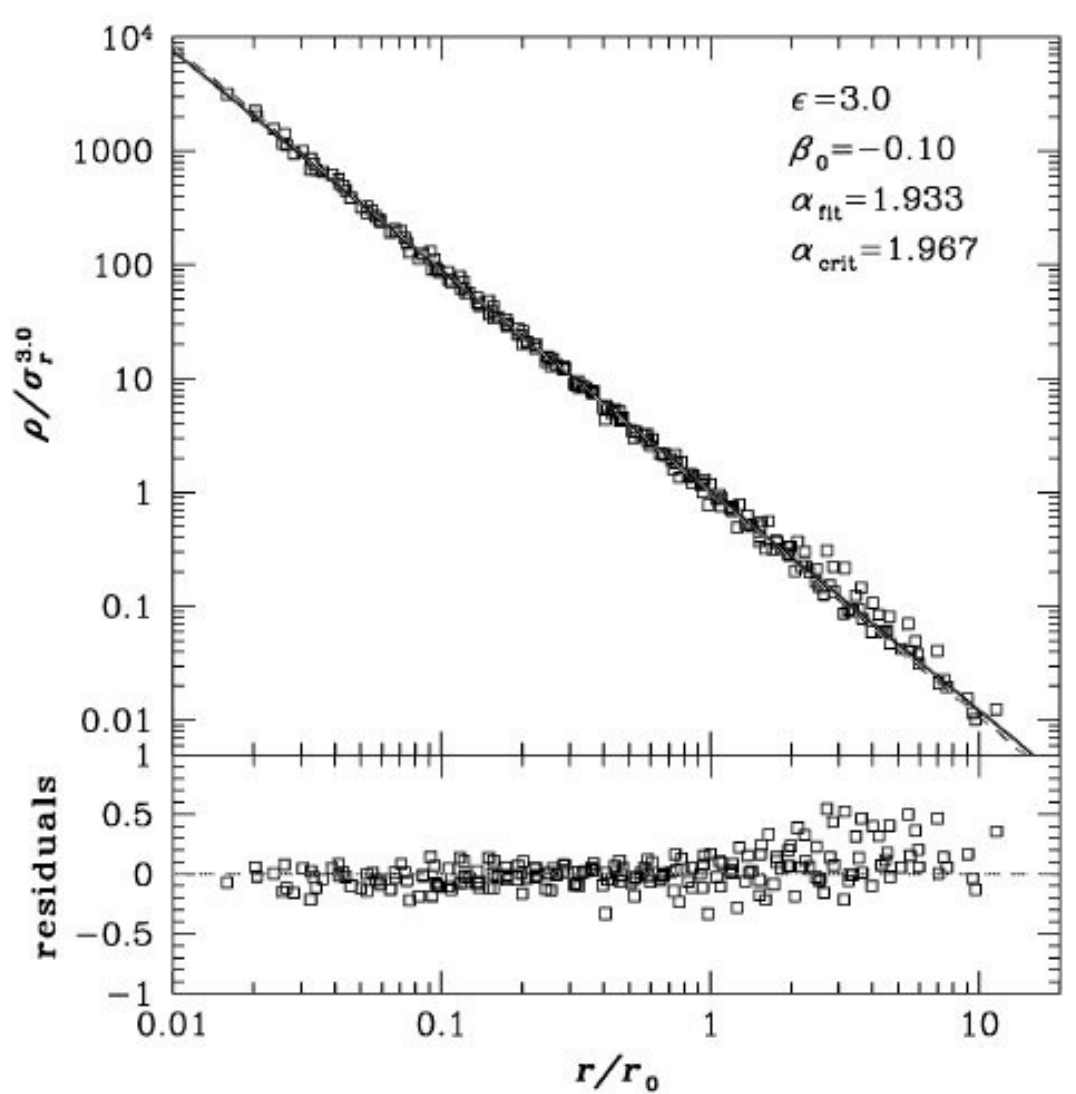


(AB+17, $z=0.06$ clusters from Ω WINGS)

Introduction

A more fundamental quantity? (Taylor+Navarro 01)

The **pseudo phase-space density profile** $Q(r) = \rho/\sigma^3$ is a power-law with radius



Its physical origin is discussed.

Lack of scale suggests
purely gravitational origin.

Maybe the result of the
violent relaxation process.

Simulations indicate it is
established very early on
in the cluster evolution
(Colombi 21)

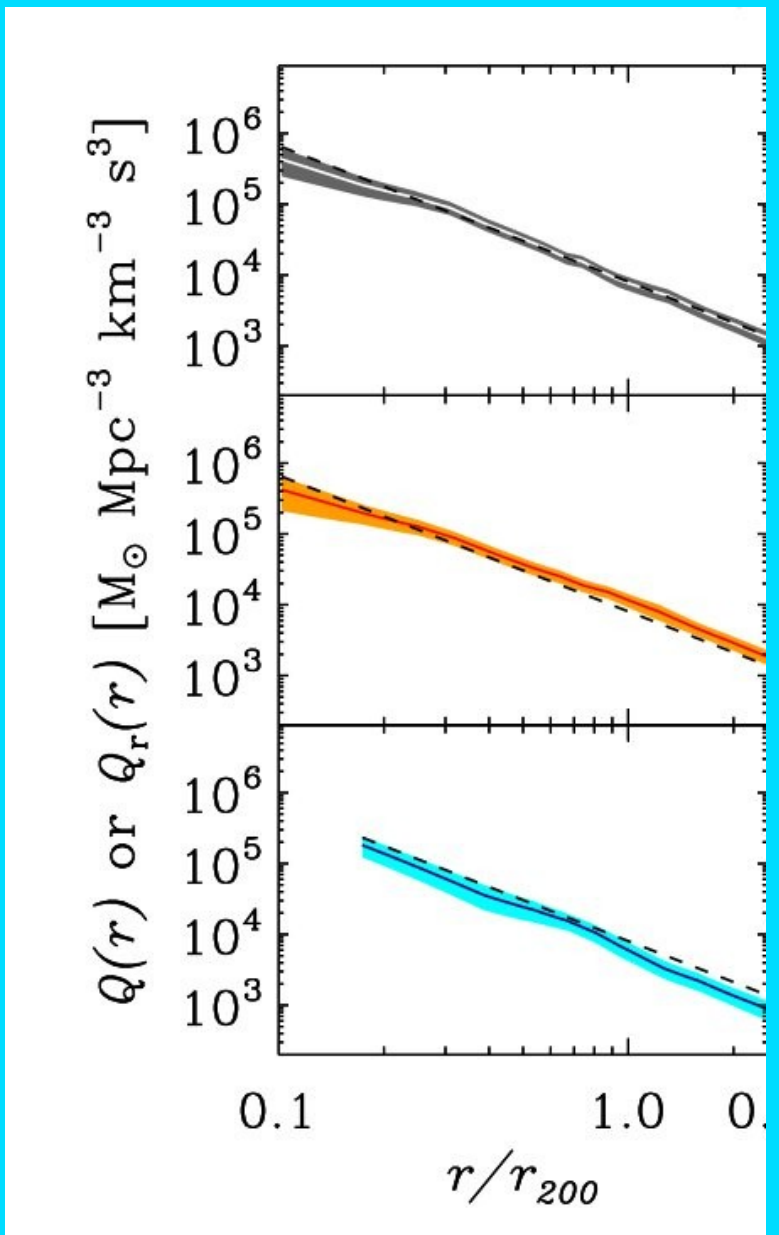
(Dehnen &
McLaughlin 05)

Introduction

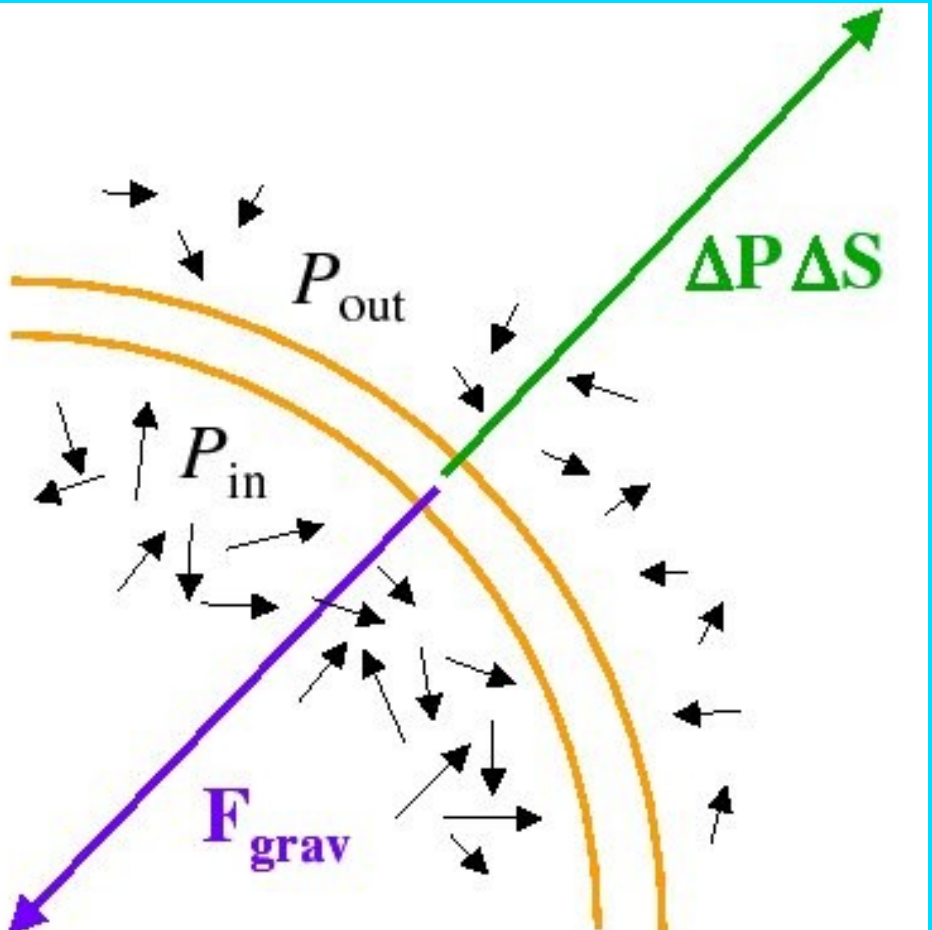
The pseudo phase-space density profile $Q(r) = \rho/\sigma^3$ has been determined for low- and intermediate- z clusters.

Agreement was found with theoretical predictions.

(AB+13)



Cluster $M(r)$ from the kinematics of cluster galaxies

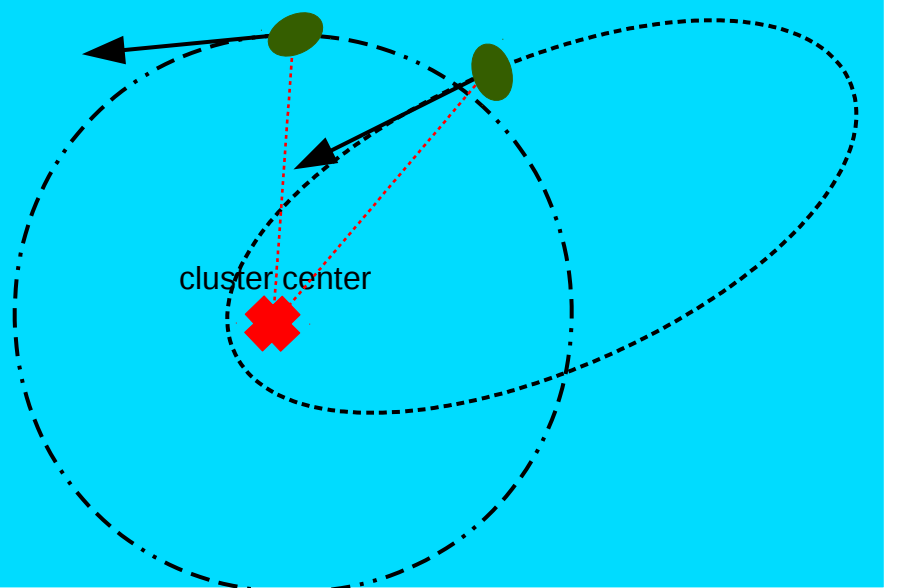


(courtesy of G. Mamon)

Cluster mass \Rightarrow Gravitational pull

Number density +
velocity distribution of galaxies \Rightarrow
Pressure against gravitational pull

Pressure is different if the velocity vector is aligned with or orthogonal to the gravitational pull, i.e. it depends on the galaxy orbital shape (radial vs. tangential)



Cluster M(r) from the kinematics of cluster galaxies: the Jeans equation

$$M(< r) = -\frac{r\sigma_r^2}{G} \left(\frac{d \ln \nu}{d \ln r} + \frac{d \ln \sigma_r^2}{d \ln r} + 2\beta \right)$$

Velocity
anisotropy
profile

$$\beta(r) = 1 - \frac{\sigma_\theta^2(r)}{\sigma_r^2(r)}$$

Mass profile

3D number
density profile

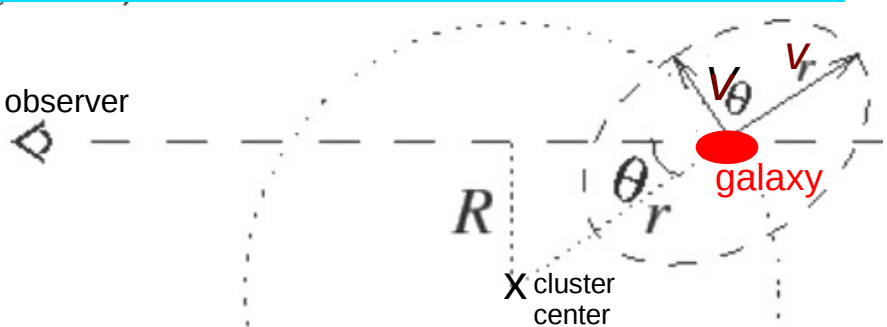
Velocity dispersion
profile along the
radial direction, r

Velocity dispersion
profile along the
tangential direction



$\beta(r)$ is related to the orbital
distribution of cluster galaxies:
 $\beta(r) < 0$ tangentially elongated
 $\beta(r) > 0$ radially elongated

The solution for the mass
profile $M(<r)$ is degenerate
with the solution for the
velocity anisotropy profile $\beta(r)$:



(courtesy of G. Mamon)

**Mass-Anisotropy Degeneracy
(aka Jeans' MADness)**

Cluster M(r) from the kinematics of cluster galaxies:

MAMPOSSt (*Mamon, AB, Boué 13*)

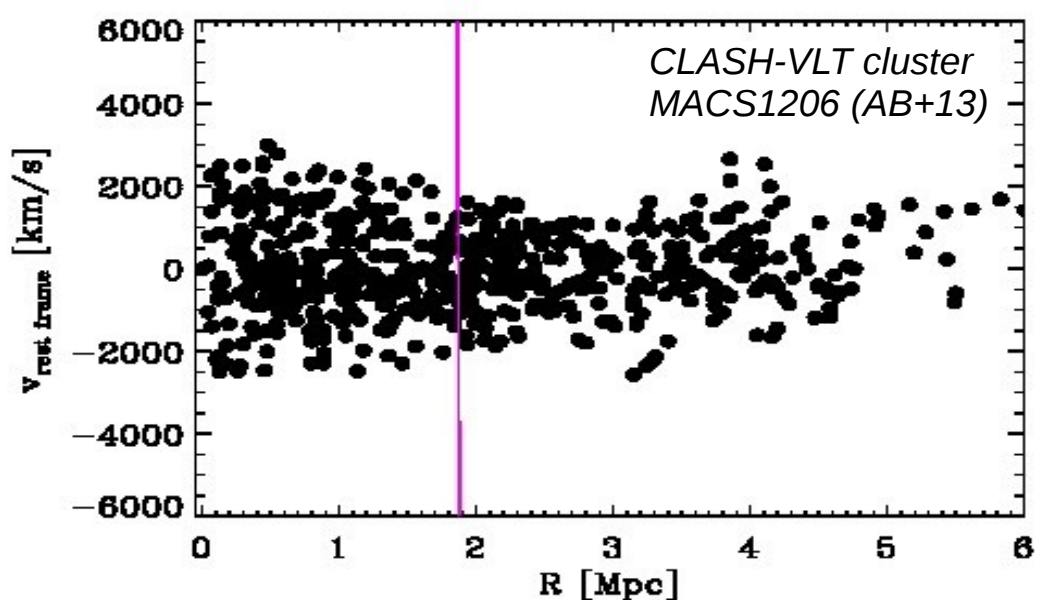
It performs a maximum likelihood fit of model $M(r)$ and model $\beta(r)$ to the projected phase-space distribution of cluster galaxies



**Modelling
Anisotropy and
Mass
Profiles of
Observed
Spherical
Systems**

Traditional approaches cannot solve the Jeans equation without making assumptions on the distribution of the orbital shapes of cluster galaxies

MAMPOSSt breaks the mass-anisotropy degeneracy of the Jeans equation by using the full information available in the spatial and velocity distributions of cluster galaxies



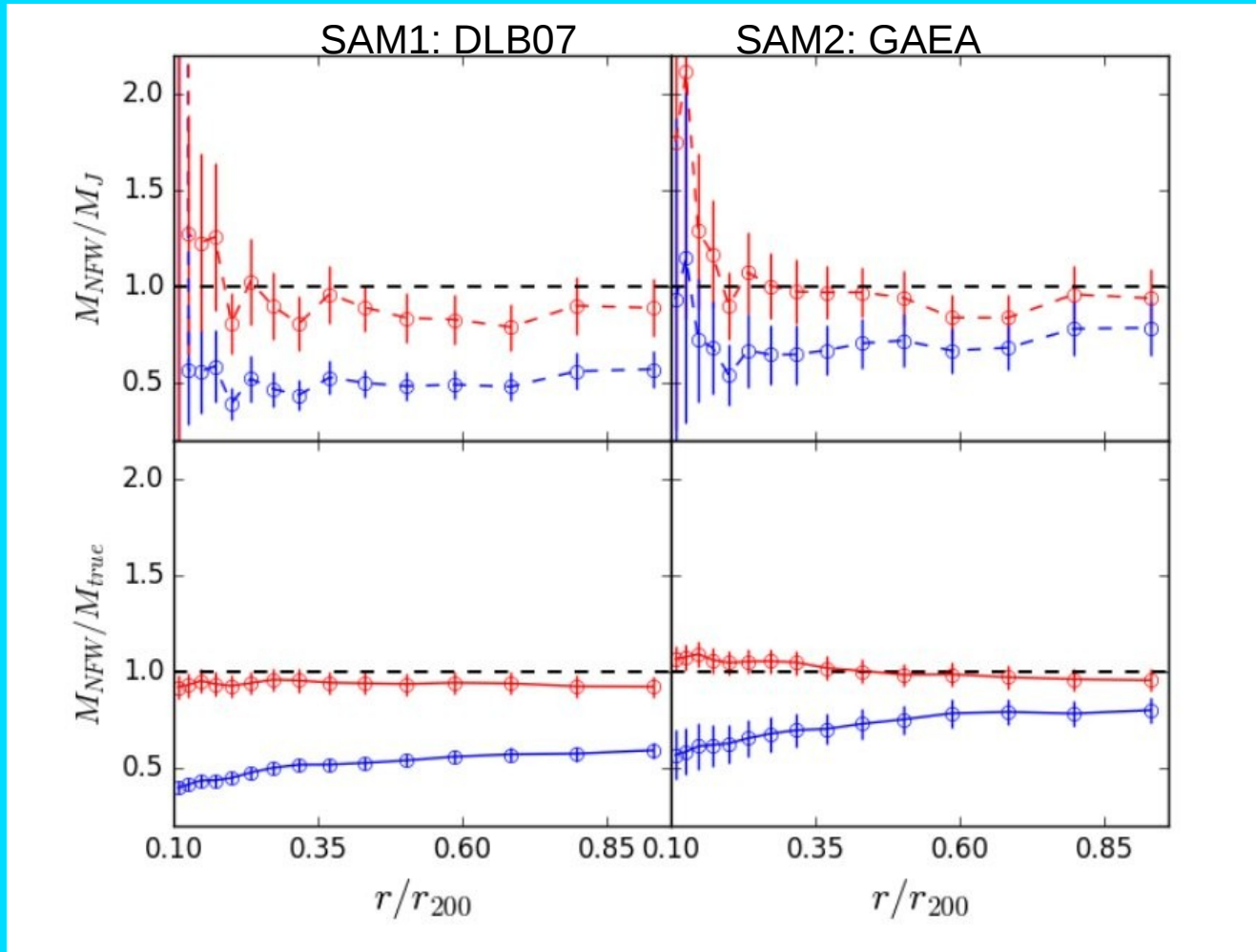
MAMPOSSt constrains $M(r)$ and $\beta(r)$ at the same time

Cluster M(r) from the kinematics of cluster galaxies:

MAMPOSSt tested vs. cluster-size halos from cosmological simulations
 - Millennium + 2 SAMs (Spergel+05; De Lucia+Blaizot 07; Hirschmann+16)

Using red
galaxies as
tracers ☺

Using blue
galaxies as
tracers ☹



(Tagliaferro, AB + 21)

Cluster M(r) from the kinematics of cluster galaxies:

MAMPOSSt constrains parameters of models:

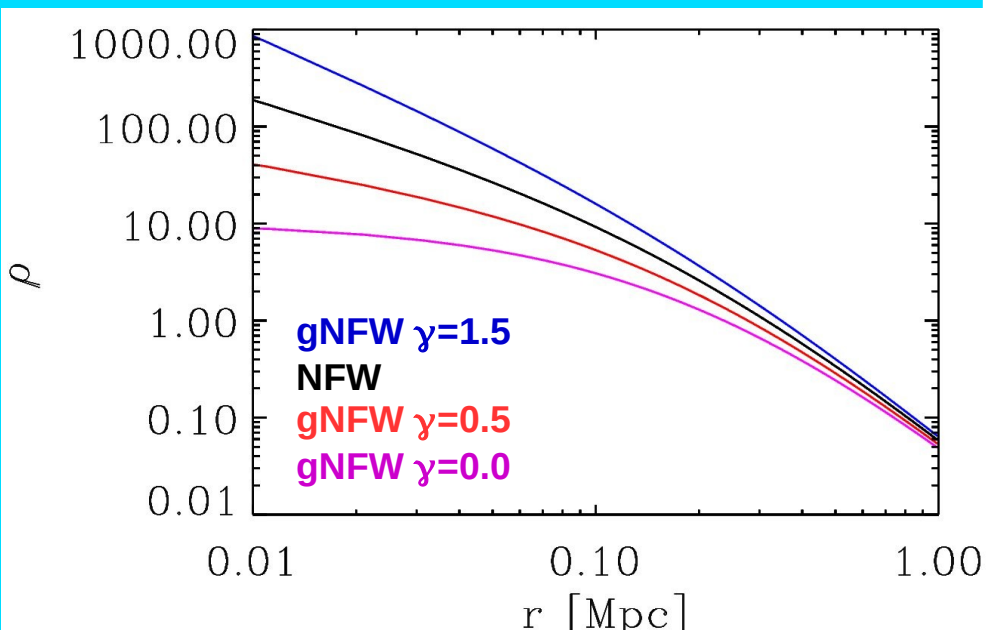
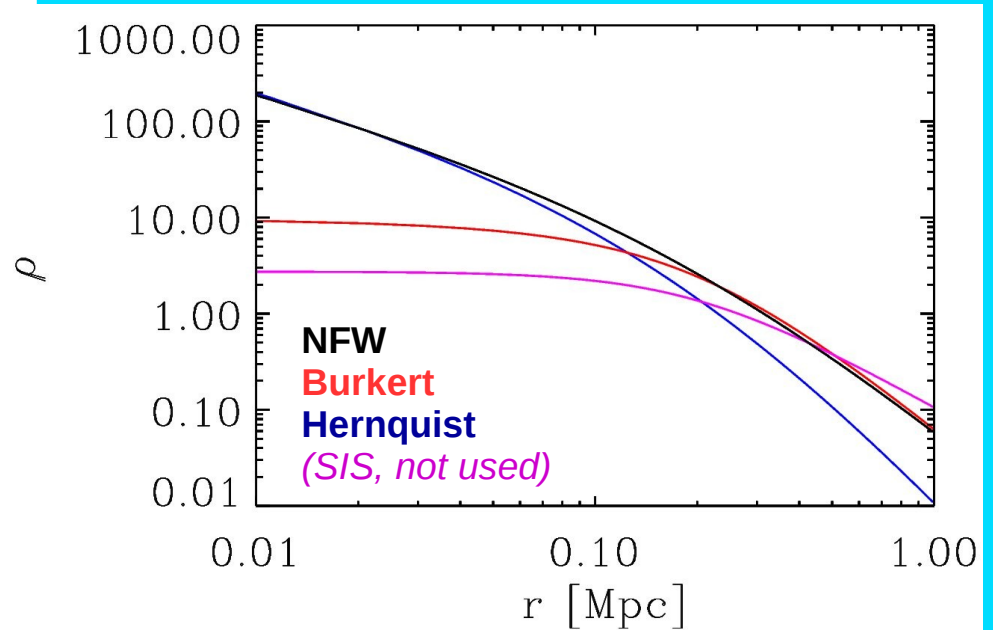
Mass $M(< r)$ models, differing for inner (outer) slope, γ_0 (γ_∞):

gNFW: $\gamma_0 = 0.0, 0.5, 1.0, 1.5$; $\gamma_\infty = 3$...generalized NFW

Burkert: $\gamma_0 = 0.0$, $\gamma_\infty = 3$...central density has a core, external slope like NFW

Hernquist: $\gamma_0 = 1.0$, $\gamma_\infty = 4$...central density like NFW, but steeper decrease at large radii

Two free parameters: M_{200} , c_{200} , or, equivalently, r_{200} , r_{-2}



Cluster M(r) from the kinematics of cluster galaxies:

MAMPOSSt constrains parameters of models:

Velocity anisotropy $\beta(r)$ models:

Constant: $\beta(r) = \beta_\infty$

Opposite: $\beta(r) = \beta_\infty(r-r_2) / (r+r_2)$...using r_2 from $M(<r)$ model

Osipkov-Merritt: $\beta(r) = r^2 / (r^2 + r_\beta^2)$

Tiret: $\beta(r) = \beta_\infty r / (r+r_2)$...using r_2 from $M(<r)$ model

Tiret-tracer: $\beta(r) = \beta_\infty r / (r+r_v)$...using r_v from galaxy number density profile

One free parameter: β_∞ or r_β

We run MAMPOSSt using:

→ $6 \times 5 = 30$ model combinations (6 $M(r)$ and 5 $\beta(r)$)

→ 3 free parameters (2 for $M(r)$ and 1 for $\beta(r)$) for each model combination

The spectroscopic data set



GOGREEN

Gemini Observations of Galaxies in Rich Early Environments

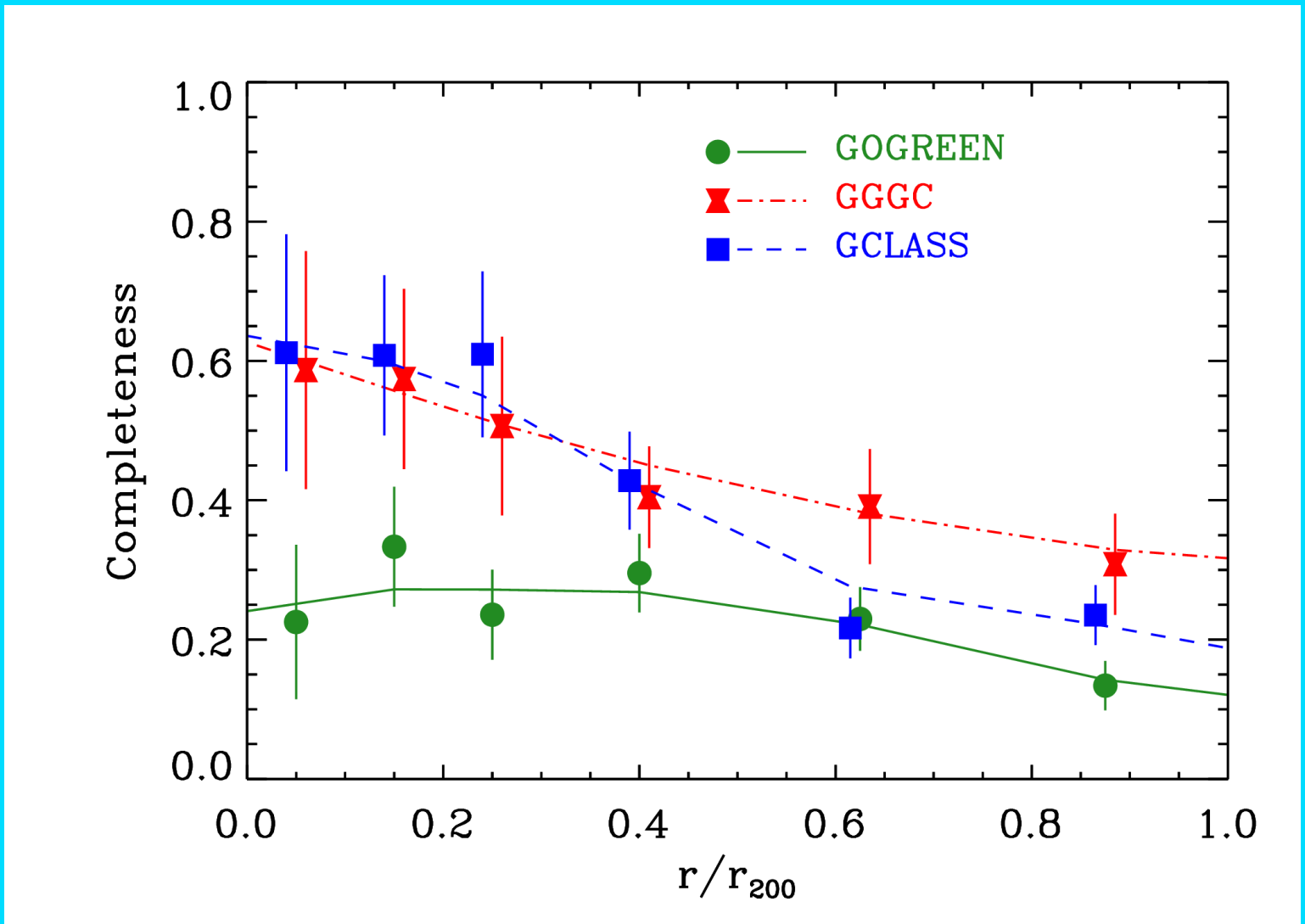
PI: M. Balogh

GOGREEN (Balogh+17, +21) : 27 clusters and groups targeted at $1 < z < 1.5$
+ GCLASS (Muzzin+12) : 10 clusters and groups targeted at $0.8 < z < 1.3$

GMOS@Gemini N+S observations,
2257 galaxies with measured velocities (+112 from the literature),
rest-frame galaxy velocity uncertainties < 154 km/s

Select only the **14** clusters with ≥ 20 spectroscopic members,
for a total of **581** members with $\log M_* \geq 9.5$, of which 467 within r_{200} ,
redshift range **0.9-1.4**,
mass range **$0.6-11 \times 10^{14} M_\odot$**

The spectroscopic data set



Spectroscopic samples completeness down to $\log M_* = 9.5$

The spectroscopic data set

Identify cluster **members** based on their positions in projected phase-space (i.e. rest-frame line-of-sight velocities vs. cluster-centric projected distances), using two algorithms:

Clean (Mamon, AB, Boué 13), based on theoretical expectations for $M(<r)$

CLUMPS (AB+21), non-parametric, based on density contrast in projected phase-space

Number of spectroscopic members per cluster ranges from 27 to 86: must **stack**

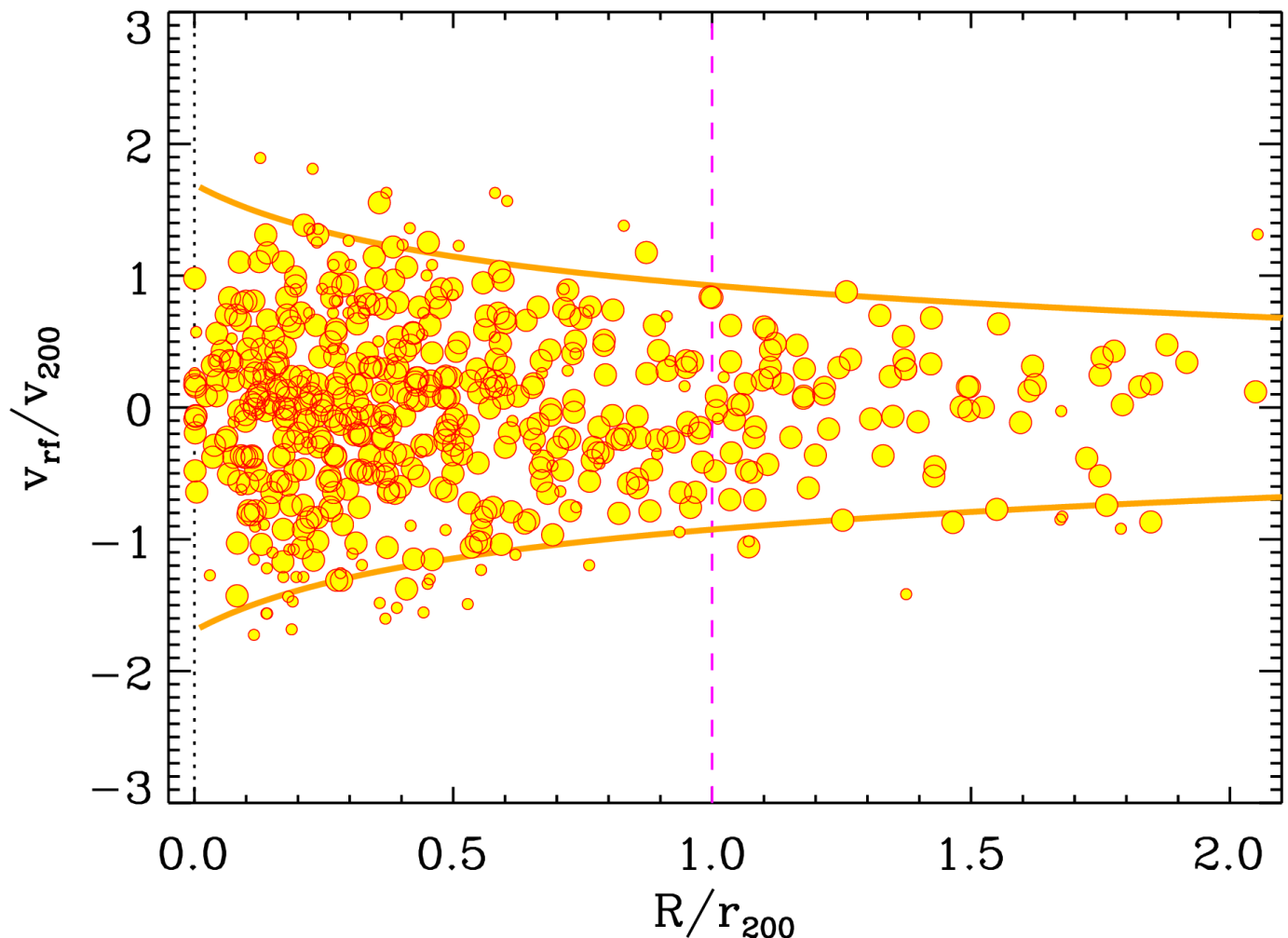
$M(<r)$ of massive clusters are predicted to be very similar (quasi-homology), use r_{200} to scale cluster-centric distances, v_{200} to scale rest-frame velocities (*this scaling is based on 1-parameter only, since r_{200} and v_{200} are related*)

Consider three different estimates of r_{200} (and v_{200}):

- from the total velocity dispersion, using a scaling relation
- from MAMPOSSt, fixing all other $M(r)$ and $\beta(r)$ parameters from theoretical studies
- from MAMPOSSt, fixing all other $M(r)$ and $\beta(r)$ parameters from observational studies

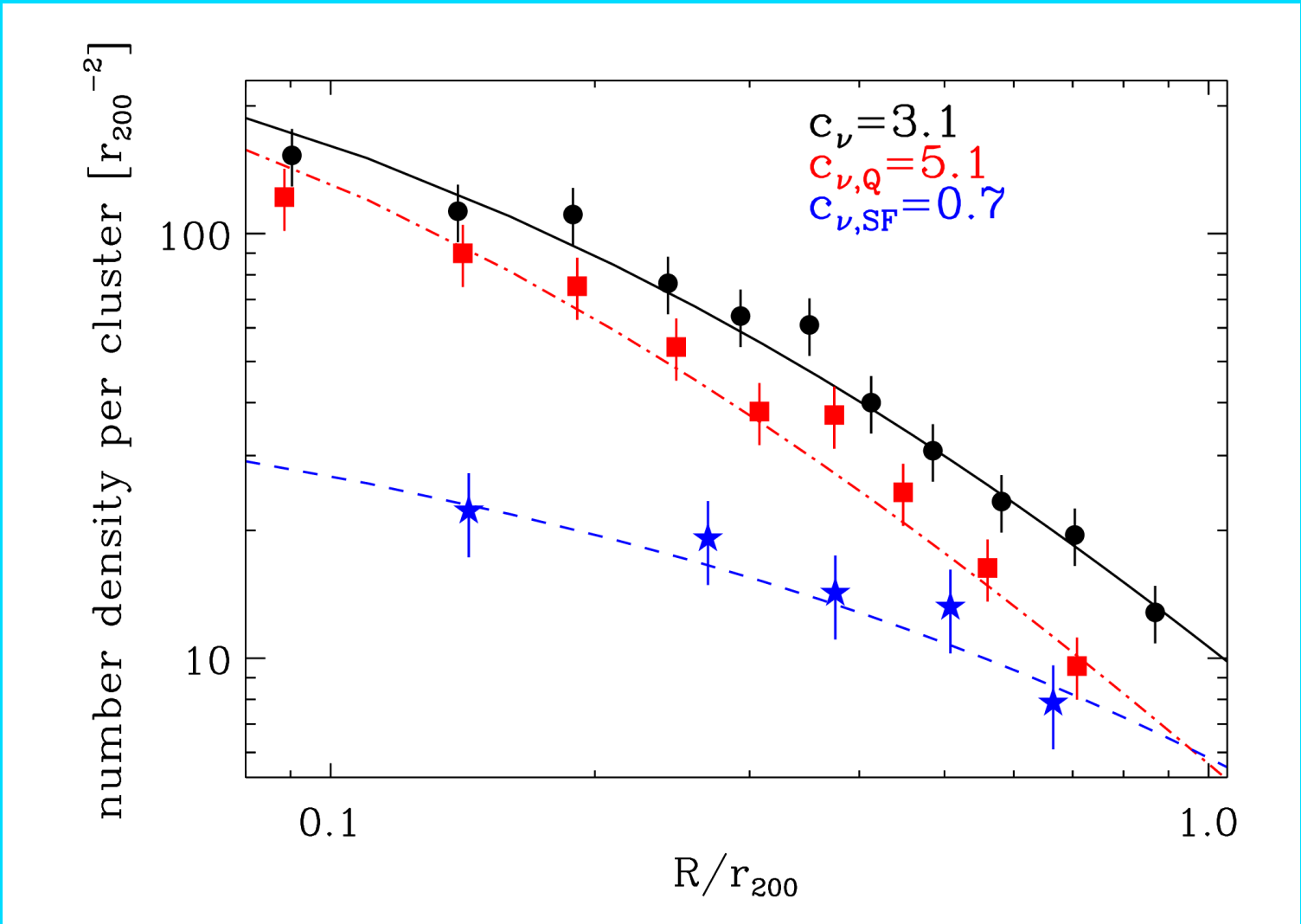
Results do not depend on the choice of the scaling

The stack cluster



Large (small) dots: membership probability 1.0 (0.5)
Escape-velocity curves assume $M(r)$ and $\beta(r)$ – for illustration purpose only

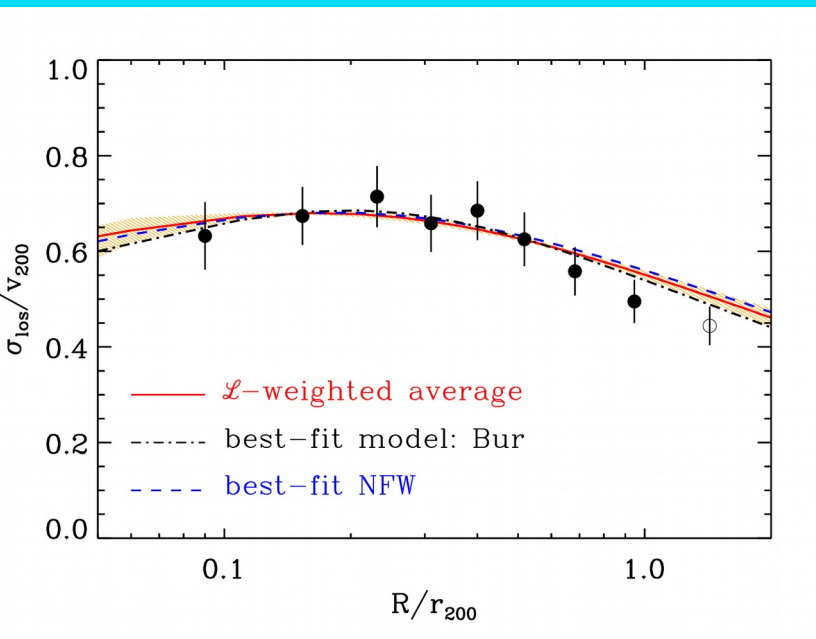
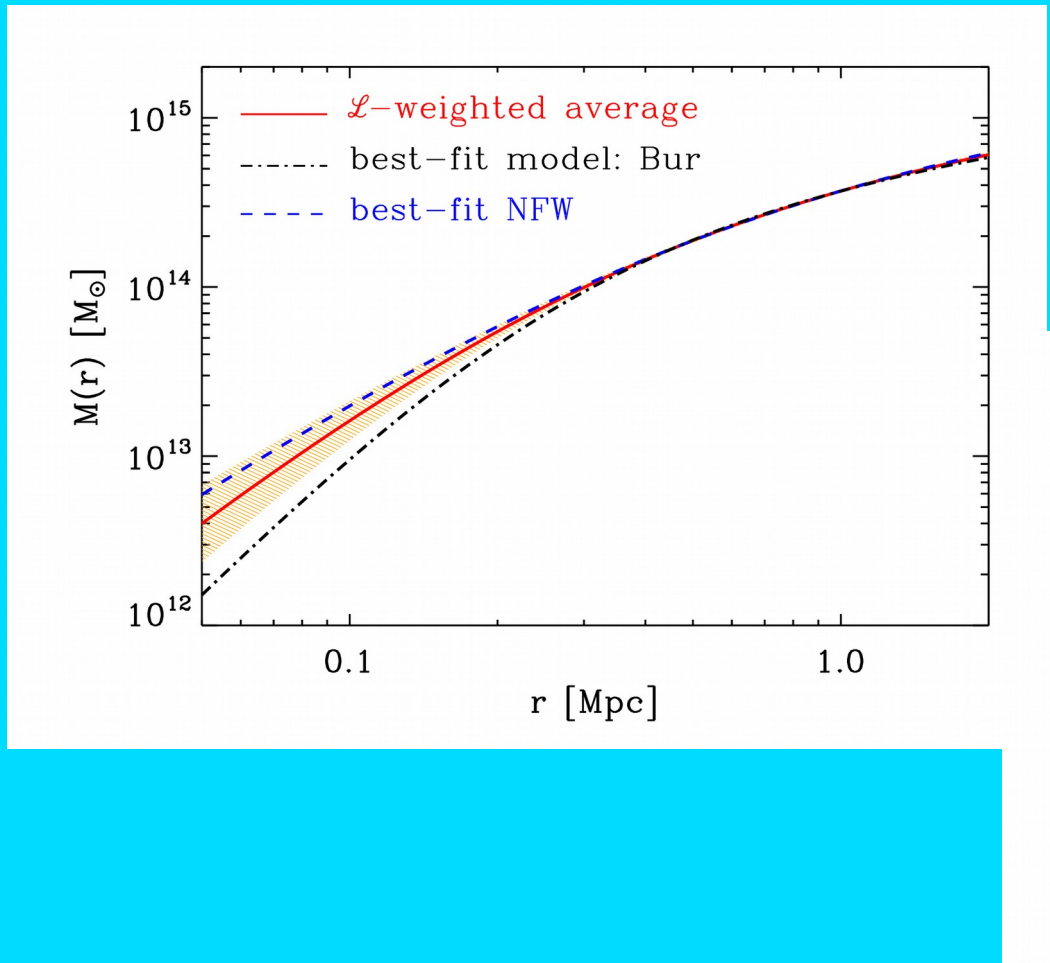
The stack cluster



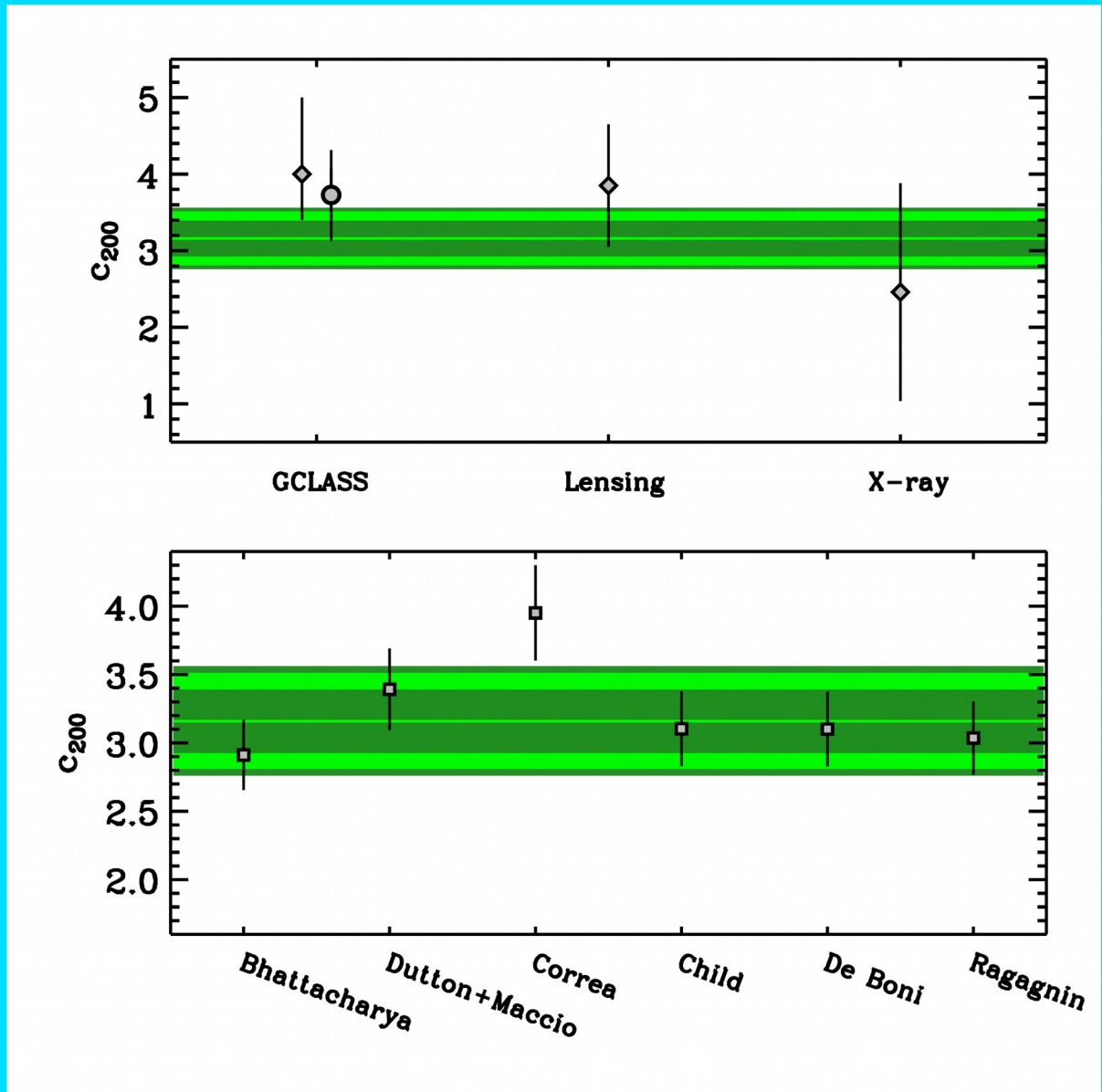
The spatial distributions of all cluster members and, separately, quiescent and star-forming members

Results: mass profile

The MAMPOSSt solution for $M(<r)$ and its projection on the line-of-sight velocity dispersion profile (to prove that it fits the data)



Results: mass profile



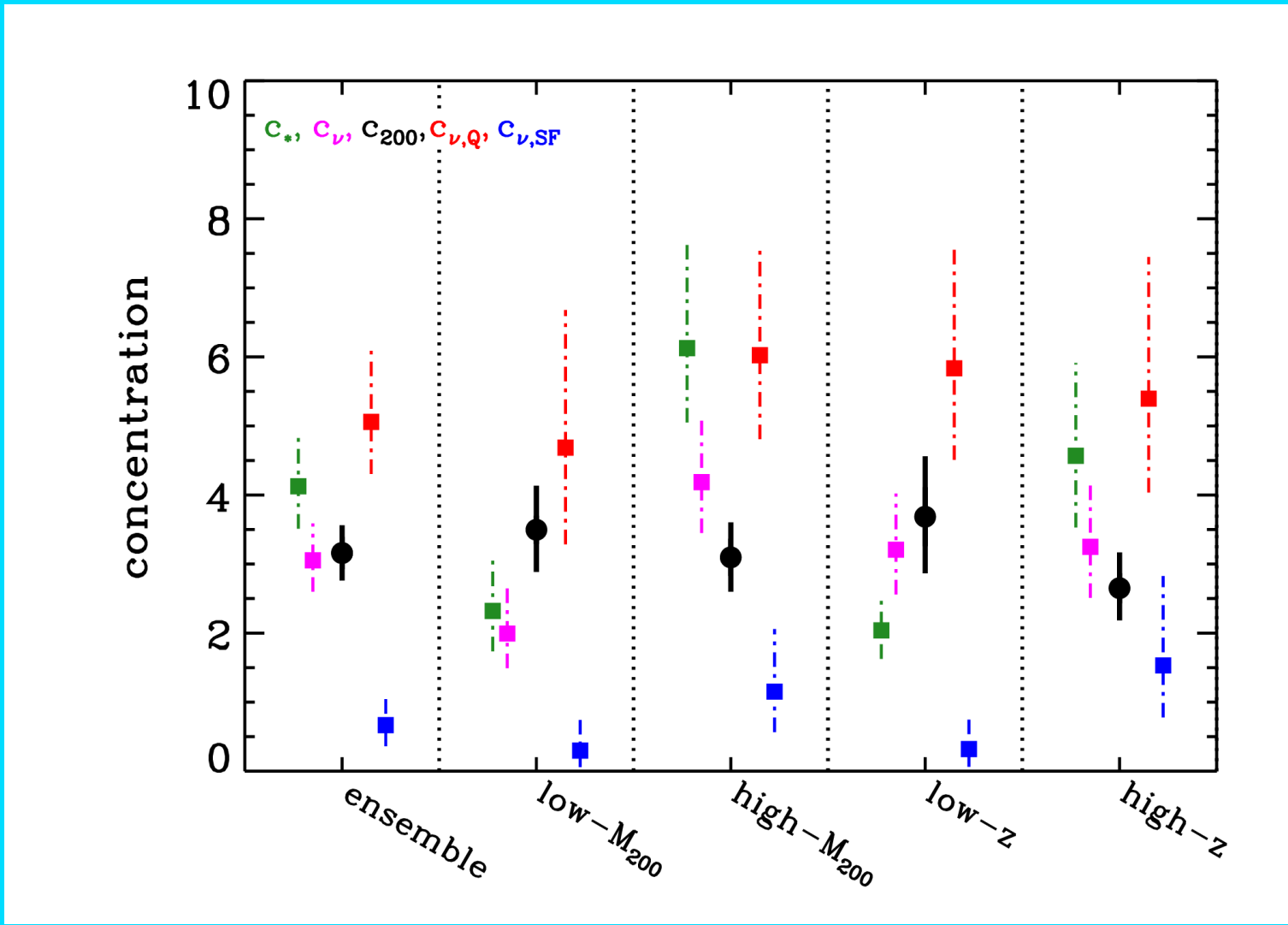
MAMPOSSt result (green shading) for c_{200} compared to:

Upper panel:
other observational results for 28 clusters in the same r_{200} and z range as the present sample
(lensing: 20 clusters; X-ray: 8;
Amodeo+16, Babyk+14, Jee+06, Jee+11, Margoniner+05, Sereno+15, Sereno+Covone 13, Groener+16)

Lower panel:
theoretical predictions from cosmological numerical simulations

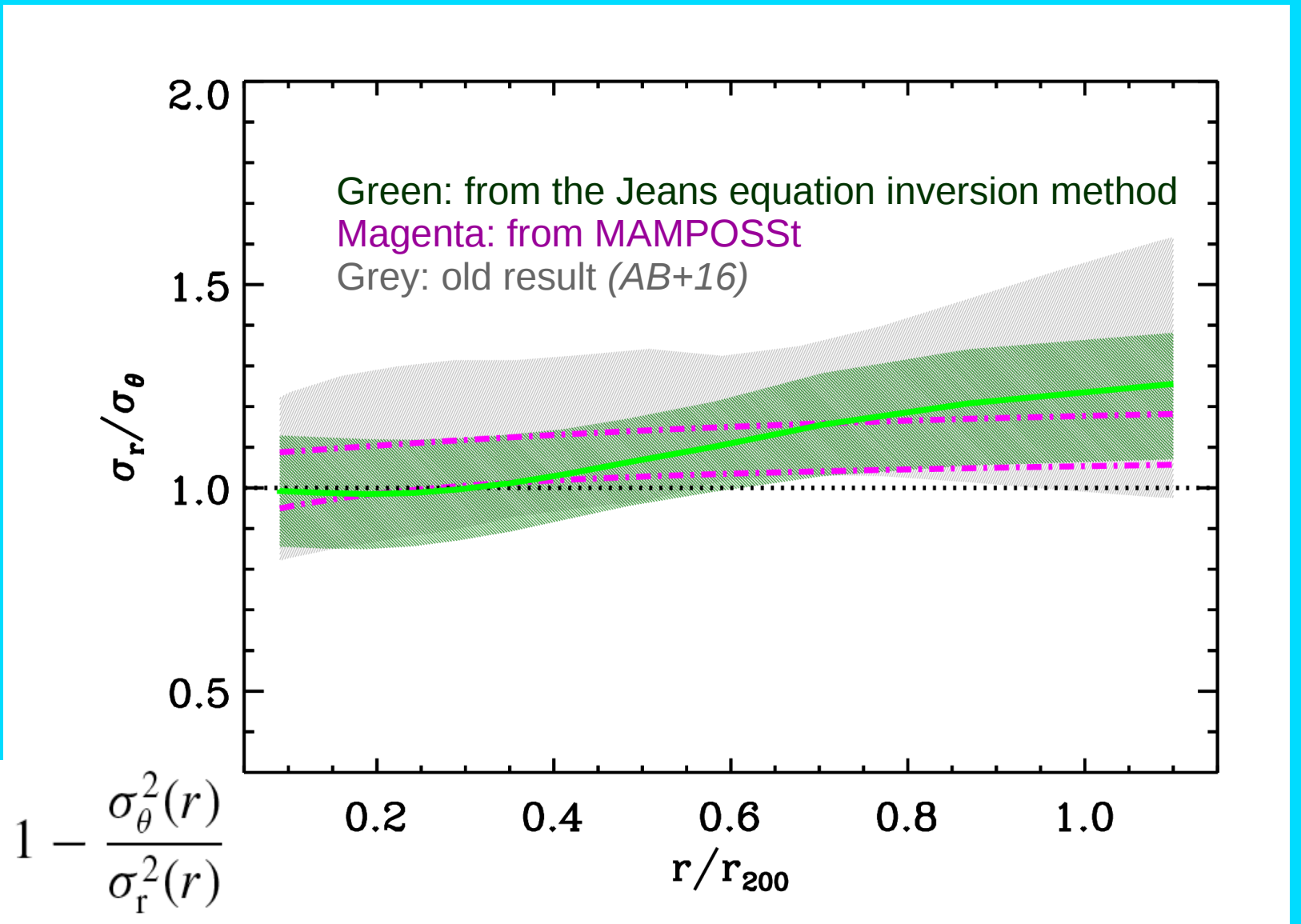
Results: mass profile

Comparing concentrations of $M(r)$ with stellar mass concentration c_* ,
and galaxy number density concentrations (c_v : all, c_{vQ} : quiescent, c_{vSF} : star-forming)



Results: velocity anisotropy profile

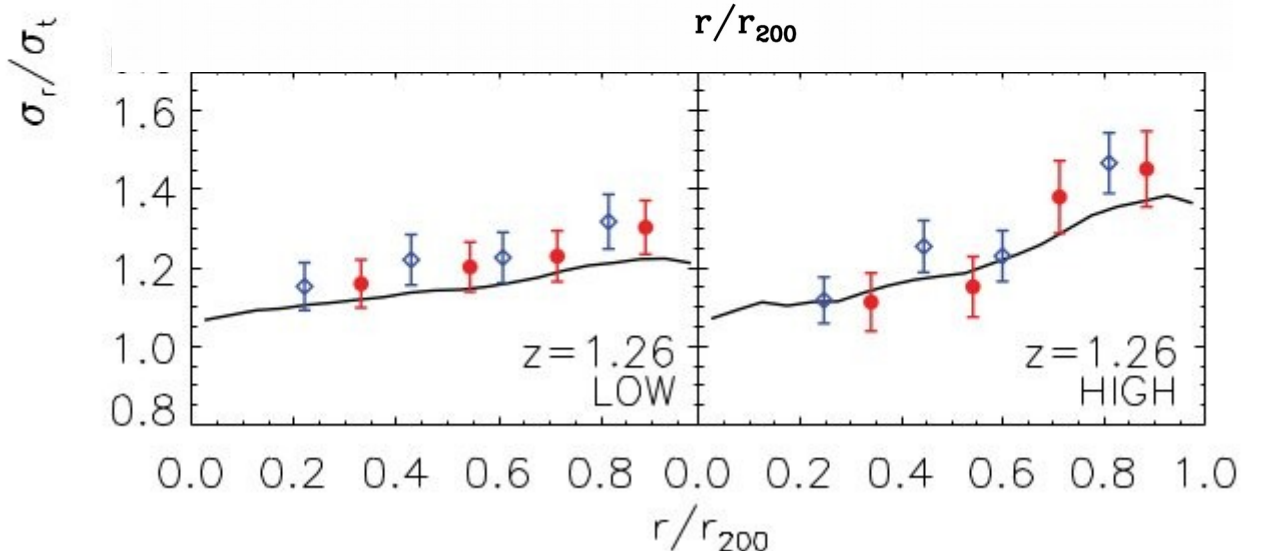
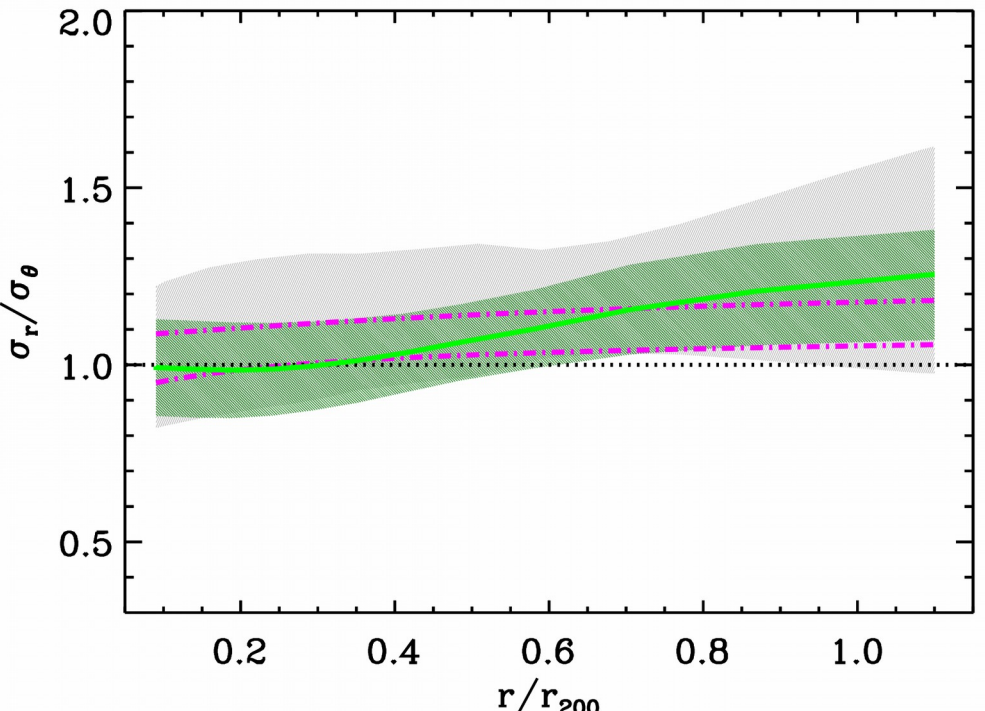
Velocity anisotropy increases with cluster-centric radius
(more radially elongated orbits outside the cluster center)



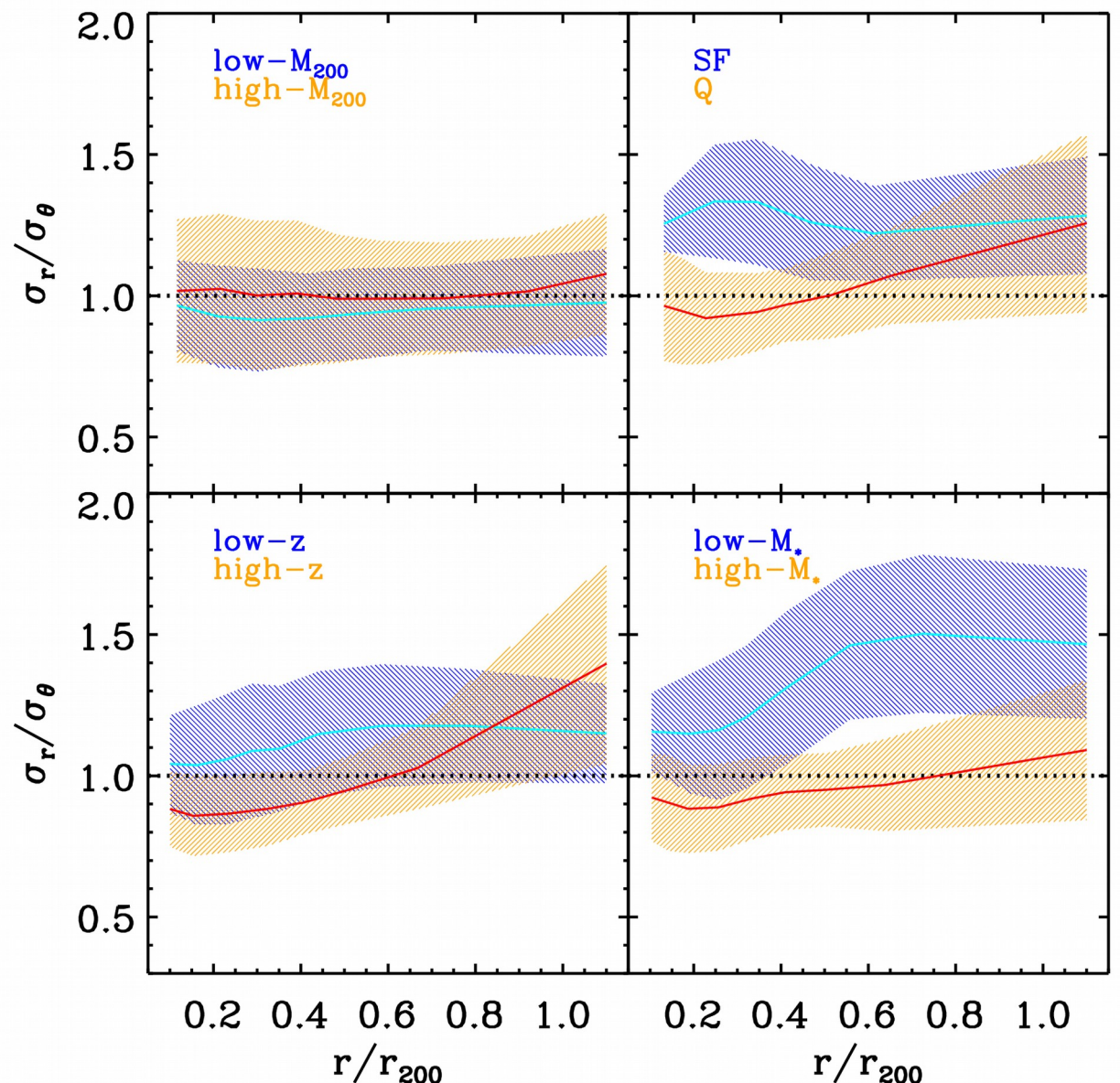
Results: velocity anisotropy profile

$$\beta(r) = 1 - \frac{\sigma_\theta^2(r)}{\sigma_r^2(r)}$$

The observed velocity anisotropy profile agrees with the profile found for cluster-size halos in cosmological simulations
(Munari, AB+13)



Results: velocity anisotropy profile

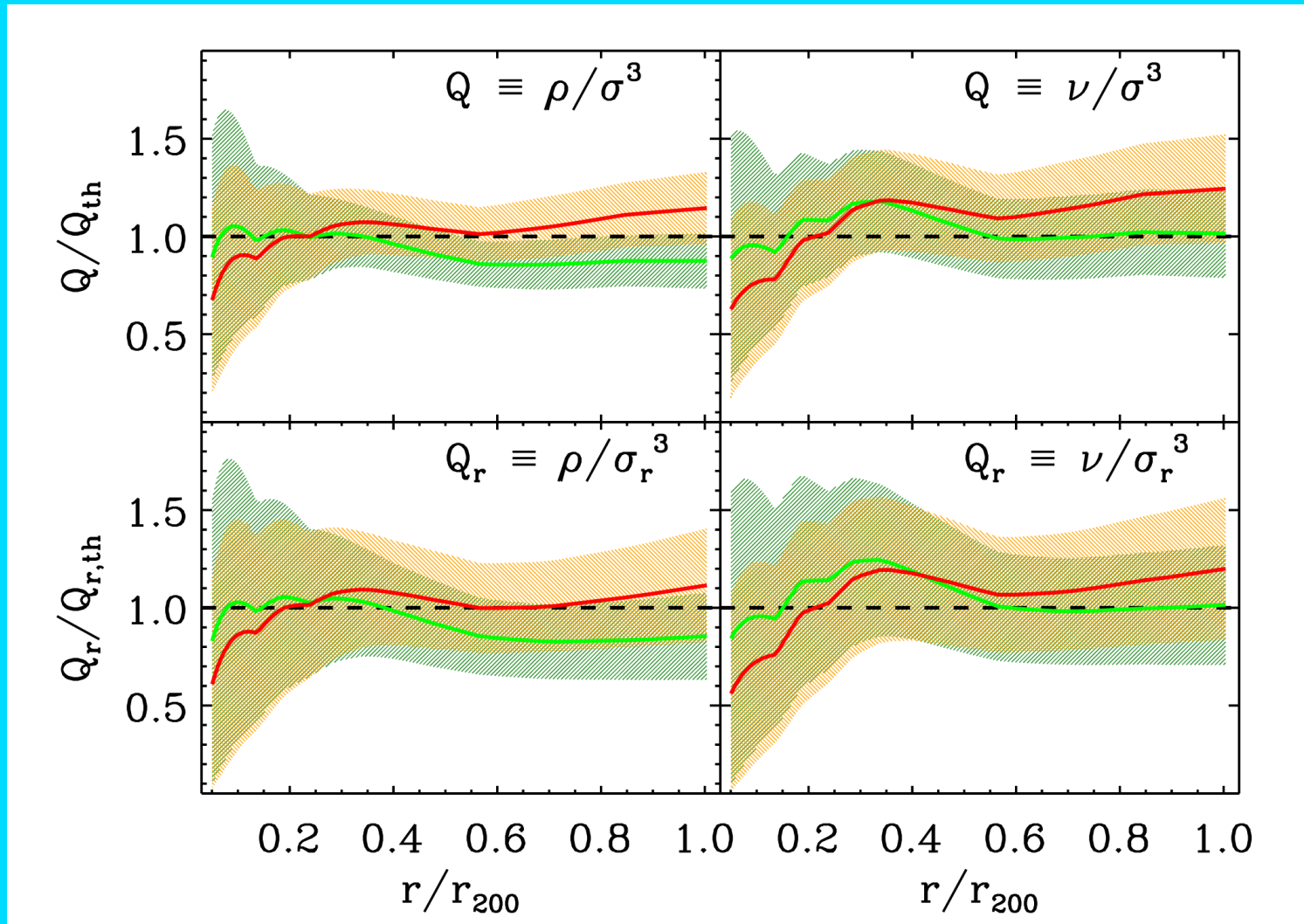


Different cluster subsamples and different galaxy populations:

Galaxies of low stellar mass are on more radial orbits than galaxies of high stellar mass

$$\beta(r) = 1 - \frac{\sigma_\theta^2(r)}{\sigma_r^2(r)}$$

Results: pseudo phase-space density profile



Observed $Q(r)$ and $Q_r(r)$ do not deviate from theoretical predictions

Results: summary

- $M(r)$ of $z \sim 1.1$ clusters consistent with theoretical expectations (NFW $c_{200} \simeq 3$); a cored profile is preferred, suggesting past AGN feedback
- Stellar mass and cluster galaxies are spatially distributed as the total mass; quiescent galaxies are spatially segregated from star-forming galaxies
- Galaxy orbits are as predicted by collective collision processes governing the central cluster region and smooth accretion processes occurring in the cluster outskirts. Galaxies of low stellar masses have more radial orbits, suggesting they join the cluster by smooth accretion, unlike galaxies of high stellar masses that experienced collective collision processes in the cluster infancy
- The pseudo phase-space density profile $Q(r)$ is consistent with theoretical expectations, confirming recent theoretical suggestions that its power-law radial behavior is established very early on in the cluster history

Discussion and prospects

Overall, clusters at $z \sim 1.1$ look very similar to nearby clusters.

Their internal structure must form rapidly in ~ 2 Gyr, since formed clusters are not observed at $z > 2$

2 Gyr \sim dynamical time at $z \sim 1.1$, suggesting collective relaxation processes (violent relaxation) as the cause of the cluster internal structure.

Clusters grow considerably in mass from $z \sim 1.1$ to $z \sim 0$, also via major mergers. Their internal structure must therefore be very resilient to merger events or it might resume in a dynamical time after the merger, that acts as a collective relaxation process.

A higher- z confirmation of this scenario could come from Euclid.